CO2-assisted propane aromatization over phosphorous-modified Ga/ZSM-5 catalysts

Journal:	*Catalysis Science & Technology*
Manuscript ID	CY-ART-12-2019-002589.R1
Article Type:	Paper
Date Submitted by the Author:	08-Feb-2020
Complete List of Authors:	Niu, Xiaoran; School of Chemical Engineering and Technology, Harbin Institute of Technology, Harbin 150001, People's Republic of China Nie, Xiaowa; Dalian University of Technology, Chemical Engineering Yang, Chun-hui; School of Chemical Engineering and Technology, Harbin Institute of Technology, Harbin 150001, People's Republic of China, Chen, Jingguang; Columbia University, Chemical Engineering

SCHOLARONE™
Manuscripts

ARTICLE

CO₂-assisted propane aromatization over phosphorous-modified Ga/ZSM-5 catalysts

Xiaoran Niu [1,2, #], Xiaowa Nie [2,3,#,*], Chunhui Yang [1,*] and Jingguang G. Chen [2,4,*]

Modification of HZSM-5 by Phosphorous (P) and Gallium (Ga) was found to enhance the activity of CO₂-assisted oxidative dehydrogenation and aromatization (CO₂-ODA) of propane to liquid aromatics products. Flow reactor studies measuring the simultaneous CO₂ reduction and the CO₂-ODA of propane were performed at 873 K at atmospheric pressure over unmodified HZSM-5 and P/Ga/ZSM-5 catalysts. At comparable propane conversion, HZSM-5 showed high selectivity toward the undesired methane product (41.4%) with a relatively low selectivity of aromatics (16.5%). In comparison, P/Ga/ZSM-5 demonstrated a significantly higher aromatics selectivity (42.3%) with a simultaneous reduction in methane selectivity (13.5%). Density functional theory (DFT) calculations identified the mechanisms for propane dehydrogenation and aromatization over P/Ga/ZSM-5 and the role of CO₂. Cooperative with P, CO₂ addition avoided the formation of molecular H₂ and reduced the barriers for benzene formation, leading to an enhanced activity and selectivity to aromatics from CO₂-ODA of propane over P/Ga/ZSM-5.

1 Introduction

Owing to the growing energy demand and increasing atmospheric carbon dioxide (CO_2) concentration, it is desirable to identify effective hydrocarbon transformation reactions in tandem with CO_2 conversion. Research on direct transformation of light alkanes into aromatics has gained considerable importance because of its potential implementation in the production of liquid fuels from C2-C4 alkanes in shale gas.[1-4] The catalytic conversion of propane into liquid aromatics with the assistance of CO_2 represents opportunities to simultaneously reduce CO_2 to CO and convert alkane into value-added products.

The medium pore HZSM-5 zeolites have been identified as active for propane aromatization but typically with low selectivity toward aromatics.[5, 6] The introduction of Platinum (Pt) into the H-ZSM-5 zeolites considerably increased the activity for the aromatization of propane.[7] However, this promoting effect of Pt was accompanied by the production of methane and ethane through hydrogenolysis of alkanes and of alkylaromatics, reducing the selectivity for the aromatics products. Zinc (Zn) or Gallium (Ga)

modified HZSM-5 catalysts were also investigated for propane to aromatic transformation, with the Zn or Ga promoters being introduced by incipient wetness impregnated,[8-11] ion exchange,[12-15] incorporation into the framework of the zeolite,[16-20] or only physically mixed.[21-24] The selectivity for aromatics was considerably improved as Zn or Ga was involved in the dehydrogenation of propane to produce alkenes that would undergo oligomerization, followed by cracking and cyclization reactions on the zeolite's Brønsted acid sites.[25-27] Both Ga and Zn ions were reported to increase the aromatics selectivity by providing active sites for the removal of hydrogen adatoms as H_2 molecule.[28,29] However, hydrogen removal still limited the aromatization rate over the Zn or Ga/ZSM-5 catalysts. Recently, Zhou et al.[30] used Pt and Fe to modify Zn/ZSM-5 to improve propane conversion and aromatics selectivity and concluded that the FePt bimetallic sites helped the $[ZnOZn]^{2+}$ sites to release the strongly adsorbed atomic hydrogen. A common issue in the above-mentioned catalysts was that the activity of the Zn or Ga modified ZSM-5 catalysts decreased with time on stream because of the coking of catalysts.[25, 31-34] Guisnet et al.[27] found that dispersed Ga facilitated the coke removal through oxidative treatment over Ga/HMFI. Samanta et al.[35] reported that Pt-modified Ga/ZSM-5 deactivated slower than Ga/ZSM-5 because the presence of Pt facilitated hydrogen spillover, resulting in the hydrogenolysis of coke precursors. Yamauchi et al.[36-38] reported that CO_2 was reduced into CO by propane concurrently converting propane as a reducing reagent into more valuable products such as aromatics. The results showed that CO_2 suppressed the by-production of ethane and the deposition of coke in the aromatization of propane over the Zn/ZSM-5 catalysts. Furthermore, Ihm et al.[39] compared the activity of propane aromatization without and with CO_2 addition over Zn/ZSM-5, and found that CO_2 could retard the catalyst deactivation but also decreased the aromatics selectivity and propane conversion.

[1] MIIT Key Laboratory of Critical Materials Technology for New Energy Conversion and Storage, School of Chemistry and Chemical Engineering, Harbin Institute of Technology, Harbin 150001, China.
[2] Department of Chemical Engineering, Columbia University, New York, NY 10027, USA
[3] State Key Laboratory of Fine Chemicals, PSU-DUT Joint Center for Energy Research, School of Chemical Engineering, Dalian University of Technology, Dalian, 116024, China
[4] Chemistry Division, Brookhaven National Laboratory, Upton, NY 11973, USA
# Authors contributed equally to this work
*Correspondence should be addressed to niexiaowa@dlut.edu.cn, yangchh@hit.edu.cn and jgchen@columbia.edu
Electronic Supplementary Information (ESI) available See

As reported in a recent work,[40] modifying Ga/ZSM-5 with Phosphorous (P) has resulted in an enhancement in hydrothermal stability and aromatics yields in CO_2-assisted oxidative dehydrogenation and aromatization (CO_2-ODA) of ethane. However, it is unclear whether such an enhancement can also be achieved for CO_2-ODA of propane. Compared to ethane, propane could be more easily activated by protons and decomposed to methane and ethylene by the protolytic C-C bond scission.[41-43] Therefore, the selectivity control for CO_2-ODA of propane should be more challenging than that of ethane. In the current study, propane aromatization was evaluated in a flow reactor with and without CO_2 over P/Ga/ZSM-5, Ga/ZSM-5 and HZSM-5 to identify the synergy between P and CO_2 during propane aromatization over P/Ga/ZSM-5. Density functional theory (DFT) calculations were performed to identify the reaction mechanisms and kinetically controlling steps of CO_2-ODA of propane over P/Ga/ZSM-5.

2 Experimental Methods

2.1 Experimental details

2.1.1 Catalyst preparation

All catalysts were synthesized with HZSM-5 containing a Si/Al molar ratio of 30 (sourced from Riogen Catalysis for Chemicals and Energy). P modification to produce P/ZSM-5 (with 0.8 wt % P) was achieved via a slurry technique by mixing the desired precursors at 313 K for 12 hours. The mixture of ethanol, water, and 85 wt % H_3PO_4 was sonicated for 10 mins before combining with a paste of HZSM-5 (mixture of 7.20 g of HZSM-5 and 20 mL of H_2O). The dried mixtures were then calcined at 823 K for 6 hours (5 K/min ramp). The incorporation of 2 wt % Ga to P/ZSM-5 was achieved via incipient wetness impregnation on 2.65 g of P/ZSM-5 with 0.28 g of $Ga(NO_3)_3 \cdot 6H_2O$ (Sigma-Aldrich) diluted in 1180 mL of H_2O. The mixture was dried overnight. And was then calcined at 563 K for 2 hours (0.8 K/min ramp) to obtain P/Ga/ZSM-5.

2.1.2 Flow reactor studies

The CO_2-ODA of propane was studied in a flow reactor at atmospheric pressure and 873 K. A sample of 50 mg of 40-60 mesh catalyst was deposited in a 4 mm quartz tube. All catalysts were pretreated with an activation period under Ar flow for 1 hour at 873 K (20 mL/min, 9.6 K/min ramp) before contacting reaction gasses, followed by additional 14 hours for steady-state experiments. The reactant gas mixture (30 vol % C_3H_8 and 30 vol % CO_2, balance Ar) was introduced with a total flow rate of 10 mL/min. The gases were analyzed with an Agilent Technologies 6890N online gas chromatograph equipped with a thermal conductivity detector (TCD) and flame ionization detector (FID) with an HP Plot Q column. Argon was used as the inert internal standard to calculate total flow rate and was the basis for quantification of product distributions. The apparent activation barrier and reaction order experiments were conducted at slightly different reaction conditions (see details in the corresponding figure captions) to minimize the effects of heat and mass transport by keeping the conversion of propane below 15%.

2.1.3 Thermogravimetric analysis (TGA) experiments

TGA experiments were conducted using a TA Instrument 8500 TGA. Approximately 12 mg of spent sample was placed onto a tared weighing pan. The spent catalyst was then subjected to a drying program in which it was ramped from room temperature to 473 K at 15 K/min and held at temperature for 5 min in the presence of Ar (40 mL/min). Then, the sample was heated to 1273 K with a 10 K/min ramp rate in the presence of O_2 (20 mL/min each).

2.1.4 Characterization of catalysts

The P/Ga/ZSM-5 catalysts were characterized and reported in detail in the previous study of CO_2-ODA of ethane.[40] In brief, X-ray diffraction (XRD) measurements revealed that the ZSM-5 crystalline structure was retained after the introduction of Ga and P. Results from X-ray absorption near-edge spectroscopy (XANES) revealed the presence of both Ga^{3+} and Ga^{1+}. The FTIR measurements of pyridine adsorption confirmed the presence of both Brønsted and Lewis acid sites in the P/Ga/ZSM-5 catalysts.

2.2 DFT details

2.2.1 Electronic structure methods

Periodic density functional theory (DFT) calculations were performed using the Vienna *ab initio* simulation package (VASP) with the ion cores described by projector augmented wave (PAW) potentials.[44-46] The exchange and correlation energies were computed using the Perdew-Burke-Ernzerh (PBE) functional within the generalized gradient approximation (GGA).[47] To consider dispersion interactions of zeolite systems, the PBE+D3 method was employed for all calculations.[48, 49] The valence electrons were expanded in a plane wave basis set with a cutoff energy of 400 eV. A Gaussian smearing with an electronic temperature of $k_B t = 0.02$ eV was applied to achieve fast convergence. The atomic structures were optimized using a damped molecular dynamics method implemented in the VASP code until the forces on all atoms were less than 0.03 eV/Å. Transition states were searched using the climbing image nudged elastic band (CI-NEB) method.[50] The minimum energy pathway was examined by interpolating 8~14 images, including the initial and final states, during transition state optimization. Each transition state was confirmed to have a single imaginary vibrational frequency along the reaction coordinate.

The adsorption energy (E_{ads}) of adsorbate is defined by $E_{ads} = E_{adsorbate-zeolite} - E_{zeolite} - E_{adsorbate}$, where $E_{adsorbate-zeolite}$ represents the total energy of the adsorbed species with the zeolite catalyst, $E_{zeolite}$ is the energy of zeolite, and $E_{adsorbate}$ is the energy of adsorbate in gas phase. A more negative E_{ads} indicates a stronger adsorption interaction. The activation barrier (E_{act}) is defined by $E_{act} = E_{TS} - E_{IS}$, where E_{TS} is the energy of transition state, and E_{IS} is the energy of the reactant associated with the elementary step. The reaction energy (E_{rxn}) is defined by $E_{rxn} = E_{FS} - E_{IS}$, where E_{FS} represents the energy of the product associated with the elementary step.

2.2.2 Computational models

The ZSM-5 zeolite model was constructed using a periodic MFI unit cell with experimental lattice constant of 20.02 Å × 19.90 Å × 13.38 Å. The Γ-point was used for all calculations. In the literature, the T12 site located in the 10-membered ring channel was reported as the most favorable site for Al substitution in the framework of ZSM-5.[51-55] The T12 site also provided sufficient space to be accessed easily by adsorbates at the intersect of the 10-membered

ring and the zigzag channel of ZSM-5, and was a common choice for Al substitution in computational studies of adsorption and reaction with ZSM-5 zeolite.[56-60] Previous studies also identified the preferential location of Al at both sites T12 and T2 in the MFI framework, leading to the formation of Al-pairs (Al12-O-Si-O-Al2) that were identified energetically favored.[52, 61] Therefore, in this work, two Al atoms were introduced into the framwork to substitute two Si atoms located at the T12 and T2 sites. A protonic HZSM-5 zeolite was constructed by adding two protons onto the bridging O36 and O13 atoms of the -Si-O-Al- framwork while for Ga/ZSM-5, the proton bound to O13 was replaced by a Ga atom. To examine whether the energetics was sensitive to the substituted sites of Al and the locations of Ga and proton, DFT calculations on the relative stabilities of different ZSM-5 models as well as the adsorption energies of propane on these catalyst models were performed. As illustrated in the **Supporting Information Fig. S1**, although the Al pair sitting positions and locations of Ga and H impacted the structural stability of ZSM-5, the energy differences of these models were not significant (< 0.2 eV). In addition, small differences (< 0.1 eV) in the adsorption energies of propane were observed, and the T12-T2(Ga) model used in this work was relatively favorable for propane adsorption. With repect to P/Ga/ZSM-5, a H_3PO_4 species was introduced into the Ga/ZSM-5 pore, which interacted with both the Brønsted acid proton of zeolite and framework O atoms by forming multiple hydrogen bonds. This species was also reported as the most possible structure of P species within the ZSM-5 pore in the literature.[62, 63] Due to the covering of the original Brønsted acid site of ZSM-5, new weak Brønsted acid site was created within the H_3PO_4 species. The optimized structures of these zeolite models are illustrated in the Supporting Information **Fig. S2**.

3 Results and discussion

3.1 Flow Reactor Measurements

3.1.1 Steady-state catalytic activity over HZSM-5 and P/Ga/ZSM-5 with and without CO_2

The conversion and product selectivity values obtained by averaging the data from 560-670 minutes on stream are listed in **Table 1**. In the absence of CO_2, HZSM-5 was not a selective catalyst for propane aromatization. The direct dehydrogenation and aromatization (DDA) of propane exhibited product distributions with 71.5% cracking products (41.4% CH_4 and 30.1% C2 products) and 16.5% liquid aromatics with a 35.8% propane conversion. Such poor aromatics selectivity indicated a facile scission of the C-C bonds of propane by the protonic sites over HZSM-5, producing more undesired methane product. Ga modification dramatically enhanced aromatics selectivity and decreased cracking activity. Propene became the dominate product with 41.7% of selectivity and the aromatics selectivity also increased to 31.1%. In the absence of CO_2, the P modification had no pronounced effect on the catalytic performance over Ga/ZSM-5 or HZSM-5.

In the presence of CO_2, the aromatics selectivity over HZSM-5 remained the same at 16.5% while propane conversion decreased. For Ga/ZSM-5, compared with that in the absence of CO_2, both aromatics selectivity and propane conversion decreased. In

comparison, the P/Ga/ZSM-5 catalyst showed high aromatics selectivity (42.3%) and low methane selectivity (13.5%) in the presence of CO_2, demonstrating the advantage in CO_2-ODA of propane.

Table 1 Catalytic flow reactor results in the presence and absence of CO_2 [a].

Catalyst	Treatment	Conversion/ %		Selectivity/ %				
		C_3H_8	CO_2	CH_4	C2 Sum	C_3H_6	C4 Sum	Aromatics liquids
P/Ga/ZSM-5	C_3-CO_2	36.1	20.0	13.5	18.3	23.4	2.5	42.3
	C_3-Ar	23.3	-	13.0	19.6	33.9	3.4	30.1
Ga/ZSM-5	C_3-CO_2	22.3	13.9	11.0	14.2	46.5	3.0	25.3
	C_3-Ar	27.5	-	9.2		41.7	3.6	31.1
HZSM-5	C_3-CO_2	29.9	15.5	41.5	32.6	7.9	1.5	16.5
	C_3-Ar	35.8	-	41.4	30.1	10.3	1.7	16.5
P/ZSM-5	C_3-CO_2	26.4	8.6	43.3	36.6	8.1	1.3	10.7
	C_3-Ar	36.7	-	41.8	28.5	9.3	1.5	18.9

[a] Values were obtained by averaging the data from 560-670 minutes on stream; Selectivity was on a C_3H_8 basis (including carbonaceous species only). For catalysts containing modifiers, the Ga and P loading were 2 wt % and 0.8 wt %, respectively and the Si/Al molar ratio for all catalysts was 30. Reaction condition: C_3H_8 (3 mL/min), CO_2 (0/3 mL/min) a total flow rate 10 mL/min at 873 K with Ar diluent (4 and 7 mL/min, respectively), 50 mg of catalyst (40-60 mesh), except for DDA of propane over HZSM-5 using 20 mg HZSM-5 diluted by 30 mg SiO_2 to achieve a comparable C_3H_8 conversion.
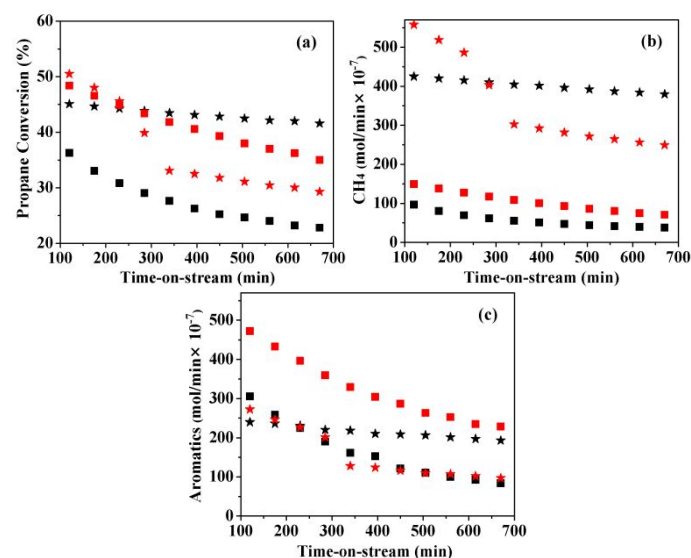

Fig. 1 Propane conversion (a) and production rates of CH_4 (b) and aromatics (c) in the reaction stream vs. time on stream for DDA (**Black** color) and CO_2-ODA of propane (**Red** color) over P/Ga/ZSM-5 (■) and HZSM-5 (★). Reaction conditions: C_3H_8 (3 mL/min), CO_2 (0 or 3 mL/min) a total flow rate 10 mL/min at 873 K with Ar diluent (7 mL/min for DDA and 4 mL/min for CO_2-ODA), 50 mg of catalyst (40-60 mesh), except for DDA over HZSM-5 using 20 mg HZSM-5 diluted by 30 mg SiO_2 to achieve a comparable C_3H_8 conversion.

Table 2 Breakdown of aromatics distribution in the presence and absence of CO_2.

Catalyst	Treatment	Benzene	Ethyl Benzene	m, p-Xylene	o-Xylene	Toluene
P/Ga/ZSM-5	C_3-CO_2	17.1	4.8	1.7	8.1	10.5
	C_3-Ar	11.6	3.0	2.0	6.0	7.6
Ga/ZSM-5	C_3-CO_2	10.3	1.9	2.2	6.7	4.2
	C_3-Ar	10.6	2.6	3.1	8.9	5.9
HZSM-5	C_3-CO_2	5.1	2.2	0.4	3.9	4.8
	C_3-Ar	7.7	1.6	0.5	2.5	4.1
P/ZSM-5	C_3-CO_2	4.4	1.1	0.3	1.8	3.2
	C_3-Ar	9.4	1.6	0.5	2.6	4.7

To better understand the catalytic behavior, the profiles of propane conversion and the production rates of CH_4 and aromatics following time on stream with and without CO_2 over HZSM-5 and P/Ga/ZSM-5 are compared in **Fig. 1**. The conversion of propane over HZSM-5 decreased significantly in the presence of CO_2, which was accompanied by a decrease in the production rates of both methane and aromatics. In the case of P/Ga/ZSM-5, the presence of CO_2 led to an increase in propane conversion and aromatics production while decreasing CH_4. From the point of view of catalyst stability, HZSM-5 without CO_2 demonstrated the least extent of deactivation among the catalysts under the reaction conditions in **Fig. 1**, although the production rate of aromatics over P/Ga/ZSM-5 remained to be higher than that over HZSM-5 after 10 hours on stream. The spent catalysts were characterized using thermogravimetric analysis (TGA) to determine the extent of coking, as shown in **Table S1**. The weight loss, normalized by propane conversion, was much lower after P modified into Ga/ZSM-5 either with or without CO_2, suggesting that P had the capability to decrease coke formation.
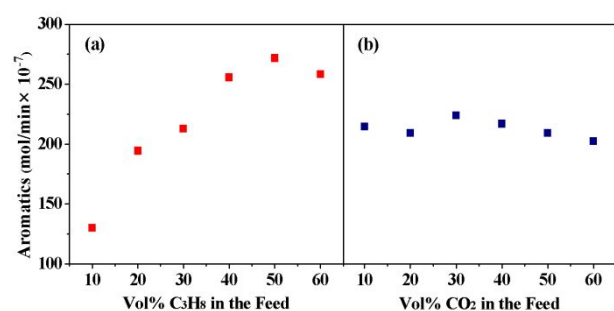

Fig. 2 Effect of the vol % of reactant C_3H_8 (a) and CO_2 (b) in the feed on the production rates of aromatics under CO_2-ODA of propane. Reaction conditions: 823 K, 50 mg of catalyst (40-60 mesh), with a total flow rate of 30 mL/min by increasing one reactant content while maintaining the other constant (30 vol%). The total flow rate remained the same by varying the Ar diluent accordingly.

3.1.2 Kinetic studies over P/Ga/ZSM-5

Kinetic studies were performed to further understand CO_2-ODA of propane over the P/Ga/ZSM-5 catalyst. Kinetic measurements were performed under conditions with propane conversion below 15% to

minimize effects of heat and mass transport, as shown in **Figs. 2** and **3**. When the concentration of propane vol % in the feed increased from 10% to 50%, the production rate of liquid aromatics (**Fig. 2a**) increased. However, it started to decrease slightly at a propane concentration of 60 vol %, suggesting that either CO_2-derived or propane-derived intermediates likely competed for the active sites in aromatics formation at high concentrations of propane. In contrast, the production rate of aromatics remained nearly constant as the CO_2 vol % increased from 10% to 60% (**Fig. 2b**), indicating that the concentration of adsorbed CO_2 (or CO_2-derived intermediates) either remained in surplus under these reaction conditions or were occupying sites that were different from those for propane activation and aromatics formation.

The apparent activation energies were estimated by measuring production rates in the temperature range of 798-823 K over P/Ga/ZSM-5, as shown in **Fig. 3**. The apparent activation barrier for propane activation was estimated to be 112 ±1 kJ·mol^{-1}, similar to the barrier for aromatics production (110 ±2 kJ·mol^{-1}). Although the apparent activation barrier for the production of propene was slightly lower (98 ±1 kJ·mol^{-1}), it suggested that propene formation was unlikely the rate-determining step. The apparent energy barrier for CO_2 activation, 115 ±7 kJ·mol^{-1}, was consistent with reported values of CO_2 activation by the metal/oxide interfacial sites in the literature, such as the value of 115 kJ·mol^{-1} for CO_2 activation at the metal/CeO_2 interfaces.[64]
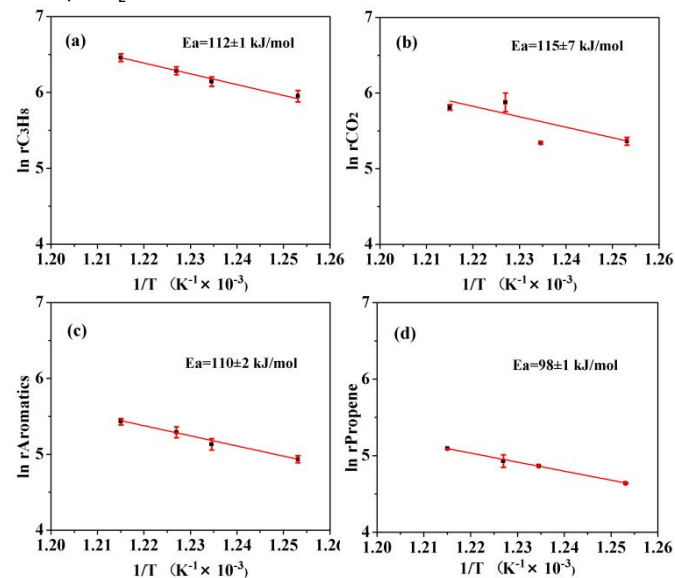
Fig. 3 Apparent activation energies derived by varying temperature over the P/Ga/ZSM-5 catalyst for C_3H_8 (a) and CO_2 (b) activation, aromatics (c) and propene (d) production. Reaction conditions: varying the reaction temperature from 798 K to 823 K, with a total flow rate of 30 mL/min (C_3H_8:CO_2:Ar = 1:1:4), 50 mg of catalyst (40-60 mesh).

3.2 Mechanistic Studies from DFT Calculations

Based on the experimental results, although modification of the HZSM-5 catalyst with Ga altered the product distribution to more propene (41.7%) and aromatics (31.1%), the promoting effect of CO_2 was only achieved after the incorporation of P into Ga/ZSM-5,

leading to a selectivity of liquid aromatics of 42.3% with a lower methane selectivity of 13.5%. To understand the mechanism and kinetically controlling steps for CO_2-ODA of propane over P/Ga/ZSM-5, DFT studies were conducted to investigate the energy pathways of propane dehydrogenation and aromatization in the absence and presence of CO_2.
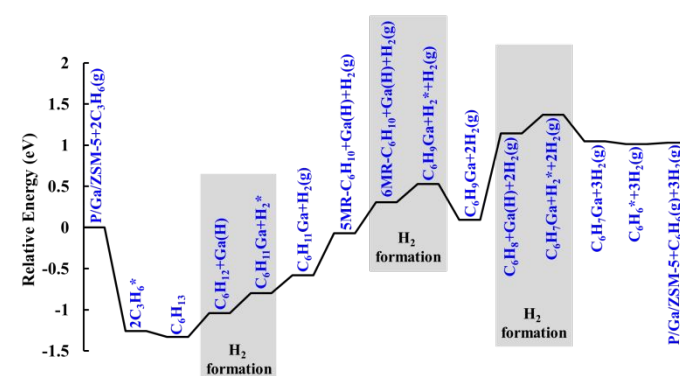
3.2.1 Propane dehydrogenation and aromatization over P/Ga/ZSM-5

On the basis of previous studies in the literatures,[65-68] the $[GaH]^{2+}$ species was identified to be the active site for alkane dehydrogenation over Ga/ZSM-5 rather than the Brønsted acid site. The transfer of Brønsted acid H in H_3PO_4 species to the Ga site had a barrier of 1.24 eV and a reaction energy of 0.31 eV (**Fig. S3**). The dehydrogenation of propane over P/Ga/ZSM-5 was investigated over the generated $[GaH]^{2+}$ site. As illustrated in **Fig. 4**, three elementary steps were involved in propane dehydrogenation to propene, i.e. (1) dehydrogenation of C_3H_8, forming an -OH with the O of H_3PO_4, (2) H_2 formation from H(O) and H(Ga), and (3) dehydrogenation of C_3H_7(Ga) to C_3H_6 coupled with the Brønsted acid site regeneration of H_3PO_4. The transition state configurations of the three elementary steps are included in **Fig. 4**, with the structures of reactant, intermediates and product given in **Fig. S4**. Both dehydrogenation steps had large barriers (1.66 and 1.76 eV for step (1) and (3), respectively), and the reaction energies were endothermic by 0.21 and 0.82 eV, respectively. The H_2 formation from H(O) and H(Ga) had a lower barrier of 0.26 eV. The effective barrier of propane dehydrogenation to propane over P/Ga/ZSM-5 predicted from DFT was 2.00 eV (**Fig. 4**). For comparison, DFT calculations were also performed for propane conversion on HZSM-5. The details are provided in the **Supporting Information**. Over HZSM-5, propane cracking was found to be kinetically more favorable than its dehydrogenation to propene due to lower barriers, resulting in methane being the dominate product. DFT calculations were consistent with the experimental results given in **Table 1** that the selectivity to methane was higher than other products such as propene and aromatics over the HZSM-5 catalyst.
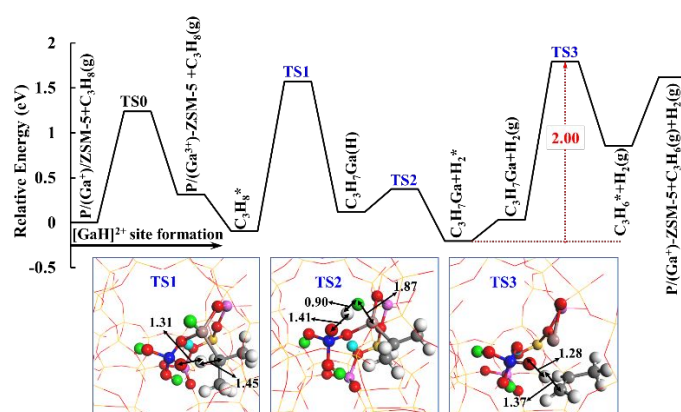
Since benzene was found to be the dominant product among the aromatics in the experimental measurements (**Table 2**), the energy pathways for propene transformation to benzene over P/Ga/ZSM-5 were calculated as an example of aromatization. The reaction energy diagram is plotted in **Fig. 5** while the optimized structures of all states involved in the path are provided in **Fig. S5**. Two propene molecules were adsorbed around the H_3PO_4 species inside the ZSM-5 pore, going through protonation, dehydrogenation, H_2 formation, five membered ring (5MR) formation, ring-isomerization of 5MR to 6MR, and H transfer, eventually leading to benzene production. Three H_2 formation steps were involved in benzene formation, which were all uphill in reaction energies, as shown in **Fig. 5**. As demonstrated in the previous work on ethane aromatization over Ga/ZSM-5 and P/Ga/ZSM-5,[40] H_2 formation reactions were found to have considerable barriers and would be slow steps in benzene formation. Therefore, the activation barriers of the three H_2 formation steps associated with propene aromatization to benzene over P/Ga/ZSM-5 were calculated and the results are given in **Fig. 6**. The dehydrogenation of the C_6H_{12} species and reaction with Ga(H) resulted in the first H_2 formation, which had a barrier of 0.55 eV. However, the barriers of subsequent C_6H_{10}+Ga(H) → C_6H_9Ga+H_2 and C_6H_8+Ga(H) → C_6H_7Ga+H_2 reactions were 2.07 and 2.31 eV, respectively, which were higher than the effective barrier (2.00 eV, **Fig. 4**) calculated for propane dehydrogenation to propene. These results indicated that propane dehydrogenation to propene should not be the rate-determining step, consistent with the experimental kinetic studies (**Fig. 3**). In the experimental results (**Table 1**), the promoting effect of CO_2 for aromatics formation was only observed after the incorporation of P into Ga/ZSMP-5. In the literature, CO_2 was considered to react with the produced hydrogen to form CO and H2O via the reverse water gas shift (RWGS) reaction and acted as a weak oxidant in alkanes dehydrogenation and aromatization.[40,69-72] Therefore, identifying the role of CO_2 in H_2 formation steps should be an important aspect for understanding the mechanism for CO_2-assisted propane aromatization. The presence of CO_2 may facilitate the reaction since the produced -H from dehydrogenation should be directly consumed through RWGS, as discussed below.
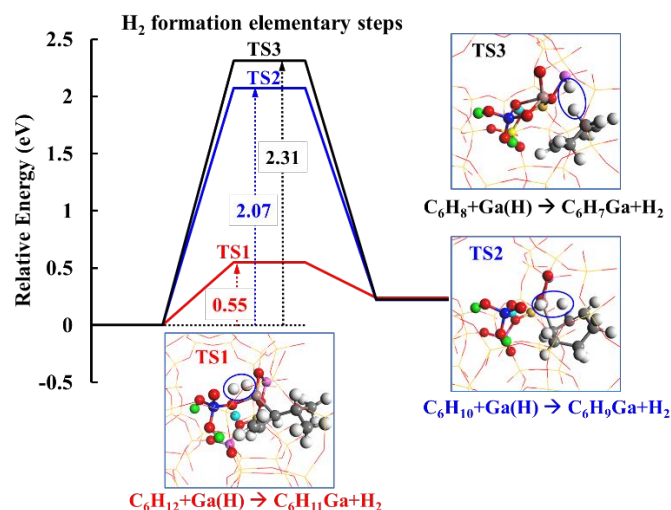

Fig. 4 Energy diagram of propane dehydrogenation to propene over P/Ga/ZSM-5 (The optimized structures of transition states generated in the path are included; the optimized structures of reactant, intermediates, and product in the path are provided in Fig. S3) (Yellow: Si, Pink: Al, Brown: Ga, Red: O, Grey: C, White: H, Bright green: H of H_3PO_4, Bright blue: H of ZSM-5, Dark blue: P).

Fig. 5 Reaction energy diagram of propene aromatization to benzene over P/Ga/ZSM-5.

Fig. 6 Energy diagrams of the three H_2 formation steps involved in propene aromatization to benzene over P/Ga/ZSM-5. Optimized structures of transition state associated with each elementary step are illustrated in the figure while the initial and final states are provided in Fig. S4.
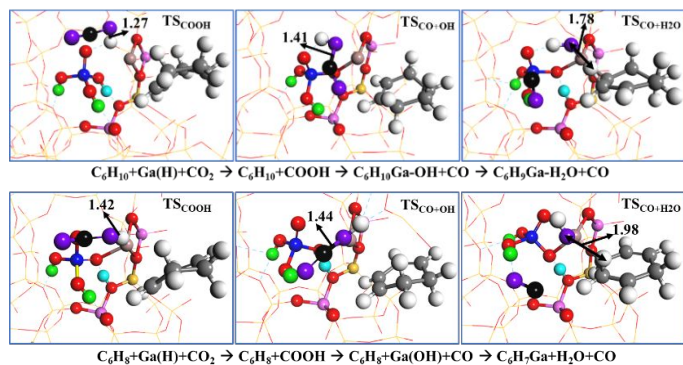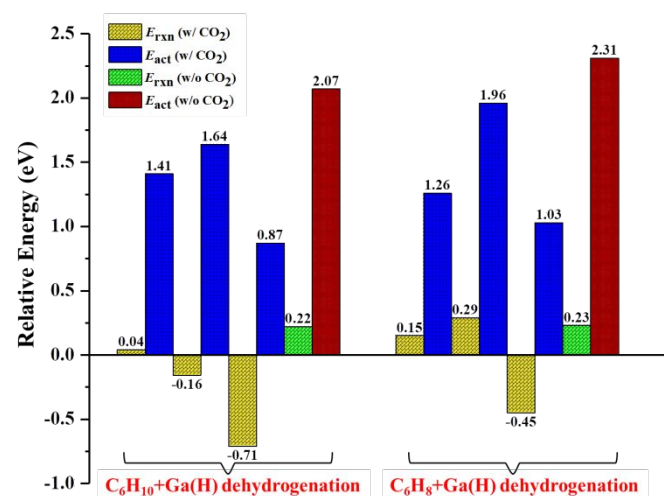

Fig. 7 Optimized structures of transition states associated with dehydrogenation of C_6H_{10}+Ga(H) and C_6H_8+Ga(H) species in benzene production over P/Ga/ZSM-5 in the presence of CO_2. (Yellow: Si, Pink: Al, Brown: Ga, Red: O, Grey: C, White: H, Bright green: H of H_3PO_4, Bright blue: H of ZSM-5, Dark blue: P, Black: C of CO_2, Purple: O of CO_2).

3.2.2 Effect of CO_2 on aromatics production over P/Ga/ZSM-5

In the presence of CO_2, the reaction mechanism and kinetic barrier of dehydrogenation of C_6H_{10}+Ga(H) and C_6H_8+Ga(H) were examined since these two steps had large barriers and formed molecular H_2 from dehydrogenation. The optimized structures of all transition states generated in these reactions are illustrated in **Fig. 7** while structures of reactants, intermediates and products are provided in **Fig. S6**. The CO_2 molecule was adsorbed around the H_3PO_4 species and reacted with the H of Ga(H) to form a COOH intermediate bound to the O atom of H_3PO_4. Then, the COOH dissociated into CO and OH(Ga) species. The reaction was completed by the transfer of H from C_6H_{10} or C_6H_8 species to OH(Ga), generating a H_2O molecule simultaneously. Thus, in the presence of CO_2, the reaction mechanism was altered and the direct formation of molecular H_2 was avoided. Most importantly, the kinetic barriers associated with elementary steps in the presence of CO_2 were decreased as compared to the case without CO_2, as demonstrated in **Fig. 8**.

Although the DFT calculated energy barriers for individual elementary steps could not be directly compared to the experimentally measured apparent activation barriers, the trends predicted from DFT agreed well with the experimental results. The introduction of P not only modified the acid site strength but also tuned the pore structure of Ga/ZSM-5, thus influencing the stability of intermediates and transition states inside the pore. The promoting effect of P addition on aromatics production from propane was enhanced when CO_2 was co-fed with propane, attributed to which the formation of H_2 molecule was circumvented and the kinetic barriers in benzene formation were reduced, demonstrating a synergy between P and CO_2. These DFT results provided mechanistic insight into the understanding of the experimentally observed CO_2-promoted aromatics production from propane over P/Ga/ZSM-5.

Fig. 8 Comparison of reaction energetics for dehydrogenation of C_6H_{10}+Ga(H) and C_6H_8+Ga(H) species in benzene production over P/Ga/ZSM-5 in the absence of CO_2 (one elementary step involved; H_2 molecule produced) and in the presence of CO_2 (three elementary steps involved; H_2 molecule not formed).

4 Conclusions

In summary, the P/Ga/ZSM-5 catalyst exhibited promising activity and stability during the process of CO_2-ODA of propane to produce liquid aromatics, demonstrating the feasibility to produce value-added liquid products from the inexpensive and abundant light alkane in shale gas while simultaneously mitigating a greenhouse gas. CO_2 enhanced the dehydrogenation kinetics while P improved the stability and tuned the acidic properties, making P/Ga/ZSM-5 a promising catalyst for CO_2-assisted oxidative dehydrogenation and aromatization of propane. Adding P should also influence the pore structure of ZSM-5, altering the formation and stability of intermediates and transition states. DFT calculations provided mechanistic insight into the understanding of the energetic pathways and kinetically controlling steps for aromatics production from propane over P/Ga/ZSM-5 and identified the important synergetic role between P and CO_2 in promoting the selectivity toward aromatics.

Conflicts of interest

There are no conflicts to declare.

References

1   G. Buckles, G. J. Hutchings and C. D. Williams, 1991, **8**, 115–123.
2   M. Guisnet and N. S. Gnep, *Appl. Catal. A, Gen.*,1992, **89**, 1–30.
3   M. V Luzgin, V. A. Rogov, S. S. Arzumanov, A. V Toktarev, A. G. Stepanov and V. N. Parmon, 2008, 4559–4562.
4   Y. Xiang, H. Wang and J. Matsubu, *Catal. Sci. Technol.*, 2018, **8**, 1500–1516.
5   Y. Ono, H. Kitagawa and Y. Sendoda, *J. Japan Pet. Inst.*, 1987, **30**, 77–88.
6   B. S. Kwak, W. M. H. Sachtler and W. O. Haag, *J. Catal.*, 1994, **149**, 465–473.
7   E. S. Publishers, N. S. Gnep, J. Y. Doyemet, F. R. Ribeiro and M. Guisnet, *Appl. Catal.*, 1987, **35**, 93–108.
8   N. S. Gnep, J. Y. Doyemet, A. M. Seco, F. R. Ribeiro and M. Guisnet, *Appl. Catal.*, 1988, **43**, 155–166.
9   G. Krishnamurthy, A. Bhan and W. N. Delgass, *J. Catal.*, 2010, **271**, 370–385.
10 P. Mériaudeau and C. Naccache, *Catal. Today*, 1996, **31**, 265–273.
11 E. G. Derouane, S. B. Abdul Hamid, I. I. Ivanova, N. Blom and P. E. Højlund-Nielsen, *J. Mol. Catal.*, 1994, **86**, 371–400.
12 H. Kitagawa, Y. Sendoda and Y. Ono, *J. Catal.*, 1986, **101**, 12–18.
13 T. Mole, J. R. Anderson and G. Creer, *J. Food Sci.*, 1985, **30**, 876–878.
14 S. B. A. Hamid, E. G. Derouane, P. Mériaudeau and C. Naccache, *Stud. Surf. Sci. Catal.*, 1994, **88**, 183–190.
15 R. L. Liu, H. Q. Zhu, Z. W. Wu, Z. F. Qin, W. Bin Fan and J. G. Wang, *J. Fuel Chem. Technol.*, 2015, **43**, 961–969.
16 M. Raad, A. Astafan, S. Hamieh, J. Toufaily, T. Hamieh, J. D. Comparot, C. Canaff, T. J. Daou, J. Patarin and L. Pinard, *J. Catal.*, 2018, **365**, 376–390.
17 G. Giannetto, A. Montes, N. S. Gnep, A. Florentino, P. Cartraud and M. Guisnet, *J. Catal.*, 1994, 145, 86–95.
18 V. R. Choudhary, A. K. Kinage, C. Sivadinarayana and M. Guisnet, *J. Catal.*, 1996, **158**, 23–33.
19 K. Nishi, S. ichi Komai, K. Inagaki, A. Satsuma and T. Hattori, *Appl. Catal. A Gen.*, 2002, **223**, 187–193.
20 M. Migliori, A. Aloise, E. Catizzone, A. Caravella and G. Giordano, *Ind. Eng. Chem. Res.*, 2017, **56**, 10309–10317.
21 N. S. Gnep, J. Y. Doyement and M. Guisnet, *J. Mol. Catal.*, 1988, **45**, 281–284.
22 G. L. Price and V. Kanazirev, *J. Catal.*, 1990, **126**, 267–278.
23 M. Guisnet and D. Lukyanov, *Stud. Surf. Sci. Catal.*, 1994, **90**, 367–378.
24 K. M. Dooley, C. Chang and G. L. Price, *Appl. Catal. A, Gen.*, 1992, **84**, 17–30.
25 Y. Ono, H. Nakatani, H. Kitagawa and E. Suzuki, 1989, **44**.
26 V. de O. Rodrigues, F. J. Vasconcellos and A. da C. Faro Júnior, *J. Catal.*, 2016, **344**, 252–262.
27 M. Guisnet and N. S. Gnep, *Catal. Today*, 1996, **31**, 275–292.
28 E. Iglesia, J. E. Baumgartner and G. L. Price, *J. Catal.*, 1992, **134**, 549–571.
29 J. A. Biscardi, G. D. Meitzner and E. Iglesia, *J. Catal.*, 1998, **179**, 192–202.
30 W. Zhou, J. Liu, L. Lin, X. Zhang, N. He, C. Liu and H. Guo, *Ind. Eng. Chem. Res.*, 2018, **57**, 16246–16256.
31 V. R. Choudhary, *Zeolites*, 1997, **18**, 188–195.
32 V. R. Choudhary, P. Devadas, A. K. Kinage, C. Sivadinarayana and M. Guisnet, *J. Catal.*, 1996, **158**, 537–550.
33 V. R. Choudhary, A. K. Kinage, P. Devadas, C. Sivadinarayana and M. Guisnet, *J. Catal.*, 1997, **166**, 380–383.
34 V. R. Choudhary, P. Devadas, S. D. Sansare and M. Guisnet, *J. Catal.*, 1997, **166**, 236–243.
35 A. Samanta, X. Bai, B. Robinson, H. Chen and J. Hu, *Ind. Eng. Chem. Res.*, 2017, **56**, 11006–11012.
36 S. Yamauchi, A. Satsuma, T. Hattori and Y. Murakami, *J. Japan Pet. Inst.*, 1994, **37**, 278–284.
37 S. Yamauchi, A. Satsuma, S. Komai, T. Asakawa, T. Hattori and Y. Murakami, *Stud. Surf. Sci. Catal.*, 1994, **84**, 1571–1578.
38 H. Tadashi, Y. Syoichi, S. Atsushi and M. Yuichi, *Chem. Lett.*, 1992, **24**, 629–630.
39 S. K. Ihm, Y. K. Park and S. W. Lee, *Appl. Organomet. Chem.*, 2000, **14**, 778–782.
40 E. Gomez, X. Nie, J. H. Lee, Z. Xie and J. G. Chen, *J. Am. Chem. Soc.*, 2019, **141**, 17771–17782.
41 M. Guisnet, N. S. Gnep, D. Aittaleb and Y. J. Doyemet, *Appl. Catal. A, Gen.*, 1992, **87**, 255–270.
42 A. Bhan and W. N. Delgass, *Catal. Rev. - Sci. Eng.*, 2008, **50**, 19–151.
43 D. B. Lukyanov, N. S. Gnep and M. R. Guisnet, *Ind. Eng. Chem. Res.*, 1994, **33**, 223–234.
44 G. Kresse and D. Joubert, *Phys. Rev. B*, 1999, **59**, 1758–1775.
45 G. Kresse and J. Furthmüller, *Comput. Mater. Sci.*, 1996, **6**, 15–50.
46 P. E. Blöchl, *Phys. Rev. B*, 1994, **50**, 17953–17979.
47 J. P. Perdew, K. Burke and M. Ernzerhof, *Phys. Rev. Lett.*, 1996, **77**, 3865–3868.
48 S. Grimme, *J. Comput. Chem.*, 2004, **25**, 1463–1473.
49 S. Grimme, J. Antony, T. Schwabe and C. Mück-Lichtenfeld, *Org. Biomol. Chem.*, 2007, **5**, 741–758.
50 G. Henkelman, B. P. Uberuaga and H. Jónsson, *J. Chem. Phys.*, 2000, **113**, 9901–9904.
51 S. R. Lonsinger, A. K. Chakraborty, D. N. Theodorou and A. T. Bell, *Catal. Letters*, 1991, **11**, 209–217.
52 E. G. Derouane and J. G. Fripiat, *Zeolites*, 1985, **5**, 165–172.
53 A. Chatterjee, T. Iwasaki, T. Ebina and A. Miyamoto, *Microporous Mesoporous Mater.*, 1998, **21**, 421–428.
54 M. S. Stave and J. B. Nicholas, *J. Phys. Chem.*, 1995, **99**, 15046–15061.
55 S. Jungsuttiwong, J. Lomratsiri. and J. Limtrakul, *Int. J. Quantum Chem*, 2011, **111**, 2275-2282.
56 D. Gleeson, *J. Comput. Aided. Mol. Des.*, 2008, **22**, 579–585.
57 T. Maihom, B. Boekfa, J. Sirijaraensre, T. Nanok, M. Probst and J. Limtrakul, *J. Phys. Chem. C*, 2009, **113**, 6654–6662.
58 S. Namuangruk, P. Khongpracha, P. Pantu and J. Limtrakul, *J. Phys. Chem. B*, 2006, **110**, 25950–25957.

59   T. Maihom, S. Namuangruk, P. Khongpracha, T. Nanok and J. Limtrakul, *ACS Natl. Meet. B. Abstr.*, 2008, 12914–12920.

60   S. Namuangruk, J. Meeprasert, P. Khemthong and K. Faungnawakij, *J. Phys. Chem. C*, 2011, **115**, 11649–11656.

61   P. J. O'Malley and J. Dwyer, *Zeolites*, 1988, **8**, 317-321.

62   Y. Chu, X. Gao, X. Zhang, G. Xu, G. Li and A. Zheng, *Phys. Chem. Chem. Phys.*, 2018, **20**, 11702–11712.

63   Y. Huang, X. Dong, M. Li and Y. Yu, *Catal. Sci. Technol.*, 2015, **5**, 1093–1105.

64   E. Gomez, S. Kattel, B. Yan, S. Yao, P. Liu and J. G. Chen, *Nat. Commun.*, 2018, **9**, 1–6.

65   M. W. Schreiber, C. P. Plaisance, M. Baumgärtl, K. Reuter, A. Jentys, R. Bermejo-Deval and J. A. Lercher, *J. Am. Chem. Soc.*, 2018, **140**, 4849–4859.

66   N. M. Phadke, E. Mansoor, M. Bondil, M. Head-Gordon and A. T. Bell, *J. Am. Chem. Soc.*, 2019, **141**, 1614–1627.

67   Y. V. Joshi and K. T. Thomson, *J. Catal.*, 2007, **246**, 249–265.

68   Y. V. Joshi and K. T. Thomson, *Catal. Today*, 2005, **105**, 106–121.

69   T. A. Bugrova, V. V. Dutov, V. A. Svetlichnyi, V. Cortés Corberán and G. V. Mamontov, *Catal. Today*, 2019, **333**, 71–80.

70   R. Koirala, R. Buechel, F. Krumeich, S. E. Pratsinis and A. Baiker, *ACS Catal.*, 2015, **5**, 690–702.

71   M. D. Porosoff, M. N. Z. Myint, S. Kattel, Z. Xie, E. Gomez, P. Liu and J. G. Chen, *Angew. Chemie - Int. Ed.*, 2015, **54**, 15501–15505.

72   M. N. Z. Myint, B. Yan, J. Wan, S. Zhao and J. G. Chen, *J. Catal.*, 2016, **343**, 168–177.

Graphical abstract
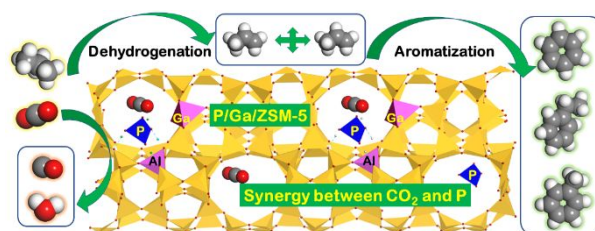
Efficient and stable phosphorous-modified Ga/ZSM-5 catalysts are identified for a one-step process of CO_2-assisted propane aromatization to liquid aromatics